ACS APPLIED MATERIALS & INTERFACES

Research Article

www.acsami.org

Phosphor-in-Glass for High-Powered Remote-Type White AC-LED

Hang Lin,[†,‡] Bo Wang,[†] Ju Xu,[†,‡] Rui Zhang,[†] Hui Chen,[†] Yunlong Yu,[†] and Yuansheng Wang[†,‡,*]

[†]Key Laboratory of Design and Assembly of Functional Nanostructures, Fujian Institute of Research on the Structure of Matter, Chinese Academy of Sciences, Fuzhou, Fujian 350002, P. R. China

[‡]Fujian Provincial Key Laboratory of Nanomaterials, Fujian Institute of Research on the Structure of Matter, Chinese Academy of Sciences, Fuzhou, Fujian 350002, P. R. China

Supporting Information

ABSTRACT: The high-powered alternating current (AC) light-emitting diode (LED) (AC-LED), featuring low cost, high energy utilization efficiency, and long service life, will become a new economic growth point in the field of semiconductor lighting. However, flicker of AC-LED in the AC cycles is not healthy for human eyes, and therefore need to be restrained. Herein we report an innovation of persistent "phosphor-in-glass" (PiG) for the remote-type AC-LED, whose afterglow can be efficiently activated by the blue light. It is experimentally demonstrated that the afterglow decay of PiG in the microsecond range can partly compensate the AC time gap. Moreover, the substitution of inorganic glass for organic resins or silicones as the encapsulants would bring out several technological benefits to AC-LED, such as good heat-dissipation, low glare, and excellent physical/chemical stability.

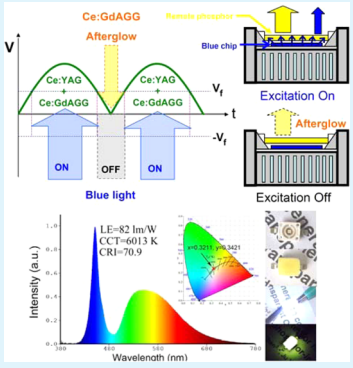

KEYWORDS: *optical materials, WLED, phosphor-in-glass, persistent luminescence, flicker effect*

1. INTRODUCTION

As one of the most active fields of research, high-powered white light-emitting diode (w-LED) lighting is currently undergoing rapid development, and will gradually replace traditional incandescent and fluorescent lamps owing to the merits of energy savings, fast switching, robustness, and environmental friendliness.[1−5] However, the price of state-of-the-art w-LED lamps is still too high, which becomes the biggest obstacle restricting the popularity of w-LED lighting. There are two key factors responsible for such high price. First, the w-LED products are commonly driven by the direct current (DC), which means the extra electro-components, including current/voltage rectifiers (or switching power supplies) and constant current sources are essential to convert the 110 V/220 V alternating current (AC) to DC and limit the current/voltage delivered to w-LEDs.[6−8] Second, in the conventional w-LED packaging procedure, the organic resin or silicone embedded with phosphors are directly coated on the chips, causing the encapsulants age easily and turn yellow due to the accumulated heat emitted from the chips, thus the thermal management, e.g., the additional heat sink, is absolutely necessary.[9−12] As a matter of fact, the applied AC-DC conversion and heat-dissipation systems totally account for 30%−50% of the LED production costs. Conceivably, searching for new techniques is urgent to realize "price-efficacy" trade-off for w-LED.

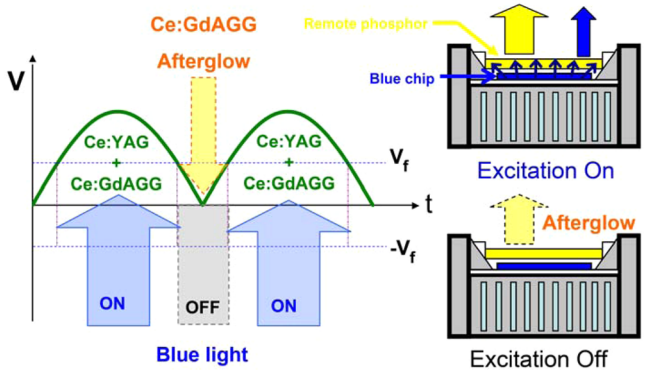

Figure 1. Proposed scheme of applying persistent Ce^{3+}:GdAGG PiG to AC-LED device with a bridge circuit design (this design is commercially used by Seoul Semiconductor Co., Ltd., making AC negative half cycle also works).

AC-LED, namely, a LED device driven directly by the city power, has received constant industrial interests since its first application as Christmas tree lighting.[13] Recently, AC-LED products (Acrich Series) manufactured by Seoul Semiconductor Co., Ltd. have been widely applied in indoor and outdoor lightings, showing advantages of not only lower price (thanking to the reduced redundant electronic components), but also higher energy utilization efficiency, more compacted volume, and longer service life than their DC-LED counterparts.[14] However, AC-LED cannot emit immediately until the voltage across the circuit is higher than its turn-on voltage (V_F),

Received: September 12, 2014
Accepted: October 20, 2014
Published: October 20, 2014

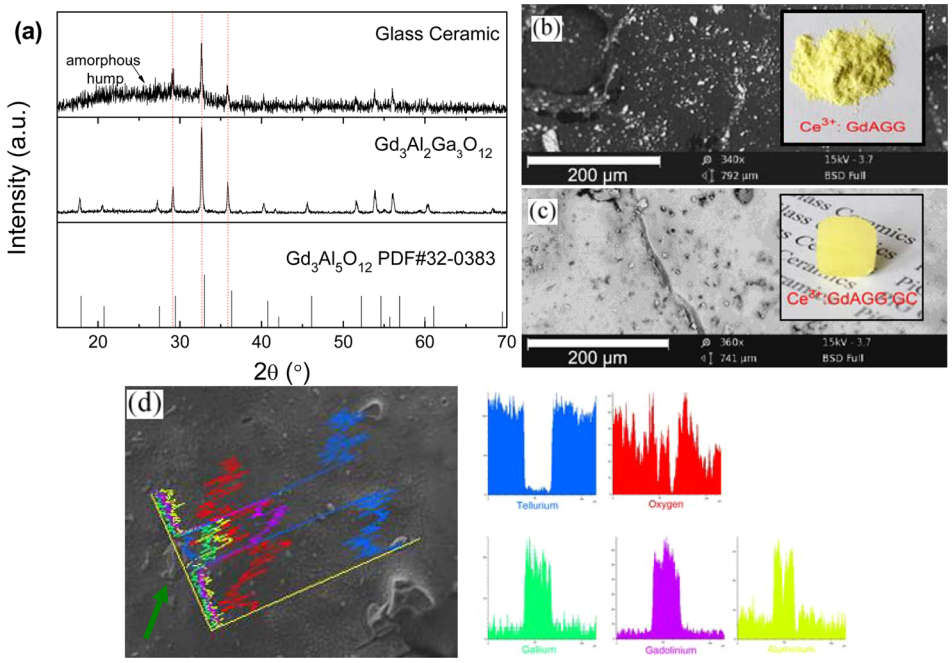

Figure 2. (a) XRD patterns, (b, c) SEM images of the GdAGG powder and the fabricated PiG containing 10% GdAGG; insets in (b, c) show photographs of the corresponding samples. (d) EDS line scan curves showing Te, Ga, Gd, Al, and O element profiles across the PiG sample.

which indicates a time gap of ~5−20 ms (a value dependent on AC frequency and the AC circuit design) is unavoidable in every AC cycle.[6] This flickering effect is not sensitive to human eyes (the duration of vision is 0.2−0.4 s), but causes visual fatigue after long period of eye use. One may solve this problem by connecting a small capacitor in series to the AC-LED circuit; unfortunately, the service life of a capacitor is limited to ~20 000 h.[6] It seems more promising to adopt a strategy of utilizing the afterglow luminescence of the persistent phosphors (e.g., Eu^{2+},Mn^{2+}:$SrSi_2O_2N_2$, Eu^{2+},Y^{3+}:$SrAl_2O_4$) to compensate the time gap, as proposed by Liu, Chen et al.[6−8] However, most persistent phosphors developed so far can only be effectively activated by the UV light,[15−18] whereas the emission wavelength of the commercial LED chip is located in the blue region. On the basis of that knowledge, we paid attention to one kind of the Ga-doped garnet-structured persistent phosphors ($RE_3Al_2Ga_3O_{12}$, RE = Y, Gd, Lu) developed first by Ueda et al. (ceramic) and then our lab (powder),[19−22] wherein Ga plays a key role engineering the host bandgap, allowing electrons' delocalization to conduction band under the blue-light excitation, and thus facilitating electrons' storage at the traps to achieve afterglow luminescence. It is expected that such blue-light-activated persistent phosphors would fulfill the requirements in AC-LED application.

Phosphor-in-glass (PiG), namely cosintering phosphors and inorganic glass at a low-melting temperature (<1000 °C), has shown its superiority as encapsulant over phosphor-in-silicone (PiS) in terms of its outstanding physical/chemical performance and good thermal conductivity deriving from the glass.[9,23,24] More importantly, PiG is known for its excellent thermal stability, which can solve the serious issues of luminous degradation and color shift causing by the yellowing and carbonizing of organic resin in PiS under long-term heat radiation.[25−28] Unlike the conventional encapsulating form that PiS directly coats on the chip, PiG is commonly designed packaging away from the chip (remote-type), which raises several important technological benefits including (1) less heat suffered by the phosphors; (2) improved light extraction efficiency by ~15%; and (3) low glare and uniform light distribution.[29−31] Most recently, a white DC-LED based on the transparent remote-type Ce^{3+}:YAG PiG phosphor has been developed in our lab,[9] which exhibits a luminous efficacy (LE) of 124 lm/W, a correlated color temperature (CCT) of 6674 K and a color rendering index (CRI) of 70. Impressively, such white DC-LED device shows admirable heat-resistant and humidity-resistant performances.

In this work, we prepared a persistent phosphor Ce^{3+}:$Gd_3Al_2Ga_3O_{12}$ (Ce^{3+}:GdAGG), whose afterglow can be efficiently activated by the blue-light; and then fabricated a PiG embedded with Ce^{3+}:YAG and Ce^{3+}:GdAGG microcrystals. This PiG was used as a remote-type phosphor to construct the white AC-LED device. The proposed scheme that the persistent PiG applies to the AC-LED is depicted in Figure 1. When the AC voltage (V_{in}) is higher than V_f, blue-light emitted from the chip excites both the Ce^{3+}:YAG and Ce^{3+}:GdAGG phosphors. The yielded yellow light blends with the transmitted blue light, resulting in the white light. When $V_{in} < V_f$, the afterglow luminescence from Ce^{3+}:GdAGG would partly compensate the AC time gap to reduce the flickering effect.

2. EXPERIMENTAL SECTION

xCe^{3+}:$Gd_{3-x}Al_2Ga_3O_{12}$ (x = 0.005, 0.01, 0.02, 0.04) powders were synthesized via a high temperature solid-state route by sintering high-purity Gd_2O_3, Al_2O_3, Ga_2O_3, and CeO_2 at 1400 °C for 4 h under 95% N_2+5% H_2 reductive atmosphere. The obtained powders were ground for subsequent use.

As reported elsewhere,[9] the initial precursor glass with compositions (mol %) of 10−30 B_2O_3, 10−30 Sb_2O_3, 5−30 TeO_2, 10−25 ZnO, 5−20 Na_2O, 0−10 La_2O_3, 0−10 BaO were prepared by using a conventional melt-quenching technique. This kind of glass, innovatively developed in our lab, is featured by its low-melting temperature to keep the phosphor powders intact. The obtained glass was further crushed and milled into powders and mixed well with the phosphors by using a ball grinder. The mixture was melted at 570 °C for 20 min with stirring to make phosphor powders distribute homogeneously as

dx.doi.org/10.1021/am506251z | ACS Appl. Mater. Interfaces 2014, 6, 21264−21269

much as possible among the glass matrix, and subsequently quenched in a copper mold to form the PiG composite. The obtained PiG was annealed at 260 °C for 5 h to relinquish the inner stress, and polished to be 1 mm thickness for optical characterizaiton.

The crystalline phases in the samples were identified by X-ray diffraction (XRD, DMAX2500, Rigaku) measurement using Cu K_α radiation source. The microstructures of the samples were studied using a scanning electron microscope (SEM, JSM-6700F, JEOL) equipped with an energy-dispersive X-ray spectroscopy (EDS) system. All the steady-state, transient-state, persistent luminescence measurements were conducted on a spectrofluoremeter (FLS920, Edinburgh Instruments). The quantum yield (QY) test was performed by using a barium sulfate coated integrating sphere that attached to FLS920. On the basis of this setup, QY is calculated by the following equation[32]

$$\eta = \frac{L_{\text{sample}}}{E_{\text{reference}} - E_{\text{sample}}} \quad (1)$$

where η represents QY, L_{sample} the emission intensity, and $E_{\text{reference}}$ and E_{sample} the intensities of the excitation light not absorbed by the reference and the sample, respectively. LE, CCT, CRI, and chromaticity coordinate of the PiG-based w-LEDs were measured in an integrating sphere of 50 cm diameter, which was connected to a CCD detector with an optical fiber (HAAS-2000, Everfine Photo-E-Info Co. Ltd.). The percent flicker of AC-LED was measured by rapid recording photometer with a sampling rate of 20 kS/s (Photo-2000F, Everfine Photo-E-Info Co. Ltd.).

3. RESULTS AND DISCUSSION

XRD curve of the 0.02Ce^{3+}:GdAGG powder shown in Figure 2a reveals the formation of pure GdAGG phase with no impurity. Compared to the standard XRD pattern of $Gd_3Al_5O_{12}$ (PDF #32−0383), the slight peak-shifting to lower angle arises from the substitution of the larger Ga^{3+} ions for the Al^{3+} ones. For the PiG sample, the GdAGG peaks are found superimposing on an amorphous hump originating from the glass matrix. SEM characterizations on a casually selected piece of PiG, exhibited in Figure 2b, c, demonstrate the size of the GdAGG particles in the glass matrix ranging from 0.5 to 20 μm, similar to those of the presynthesized GdAGG powders, indicating that the glass-melting procedure does not influence the GdAGG microstructure significantly. It is also found that the GdAGG particles distribute homogeneously in the glass matrix, with no agglomeration. The EDS line scan across the indicated particle, shown in Figure 2d, confirms its composition, i.e., Gd, Al, Ga, O. As a comparison, the glass component Te signal is only detected in the glass matrix. The O signal is originated from both the particle and the glass matrix.

The photoluminescence excitation (PLE) and photoluminescence (PL) spectra of the 0.02Ce^{3+}:GdAGG powder and the fabricated 0.02Ce^{3+}:GdAGG PiG are shown in Figure 3a, both exhibiting the typical Ce^{3+}:4f↔5d broadband excitations (peaked at 350 and 450 nm) and emissions (peaked at 550 nm).[33,34] The excitation band peaked at 275 nm in the powder sample comes from the Gd^{3+}:$^8S_{7/2} \rightarrow {}^6I_J$ transition. For the PiG sample, the 275 nm band disappears and the 360 nm one weakens, probably caused by the absorption of glass matrix in the short-wavelength region (please refer to the transmittance spectrum of the glass in Figure S1 in the Supporting Information). The luminescent dynamical study and QY measurement in Figure S2 in the Supporting Information reveal that the luminescent property of Ce^{3+} keeps almost unchanged after incorporating Ce^{3+}:GdAGG crystals into glass, implying that the glass-melting induced interdiffusion between the GdAGG crystals and the glass matrix is negligible,

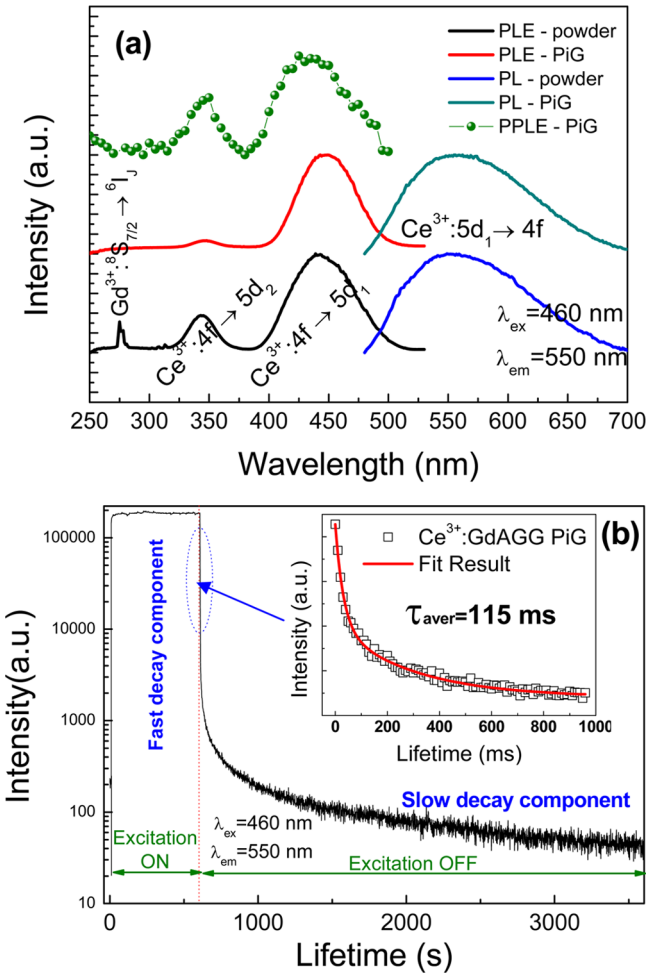

Figure 3. (a) PLE, PL, PPLE spectra of Ce^{3+}:GdAGG powder and PiG. (b) Afterglow luminescence decay curve of Ce^{3+}:GdAGG PiG excited at 460 nm and monitored at 550 nm; inset in b shows the initial 1s decay at a step of 10 ms after the stoppage of excitation source. The creation of PPLE spectrum was calibrated for the spectral distribution of the exited light, assuming that the intensity of the afterglow is proportional to the flux of the excited light.

otherwise, the released Ce^{3+} ions would disperse into glass and exhibit totally different spectral features with a lower QY, since Ce^{3+}:5d electrons are very sensitive to the local environment. To evaluate the persistent performance of the fabricated $x$$Ce^{3+}$:GdAGG ($x$ = 0.5, 1.0, 2.0, 4.0%) PiGs, we recorded afterglow luminescent decays of the samples after ceasing the 460 nm excitation, as presented in Figure S3 in the Supporting Information, wherein the 2.0% Ce^{3+}:GdAGG sample yields most intense initial afterglow brightness. Figure 3b reveals that the afterglow decay curve comprises a fast decay component and a slow one (lasting even for 1h). In the fast decay process, the afterglow luminescence is bright, whereas in the slow decay process it becomes very weak. By carefully measuring the sample in the initial 1s decay at a step of 10 ms, as presented in the inset of Figure 3b, the curve could be well-fitted with an average lifetime of 115 ms, indicating its potential to compensate the AC time gap. To reveal the effectiveness of the excitation wavelength for afterglow luminescence, the persistent photoluminescence excitation (PPLE) spectra were measured and created by plotting the afterglow intensities at 50 ms after the stoppage of excitation versus the excitation wavelength in Figure 3a, following the method proposed by

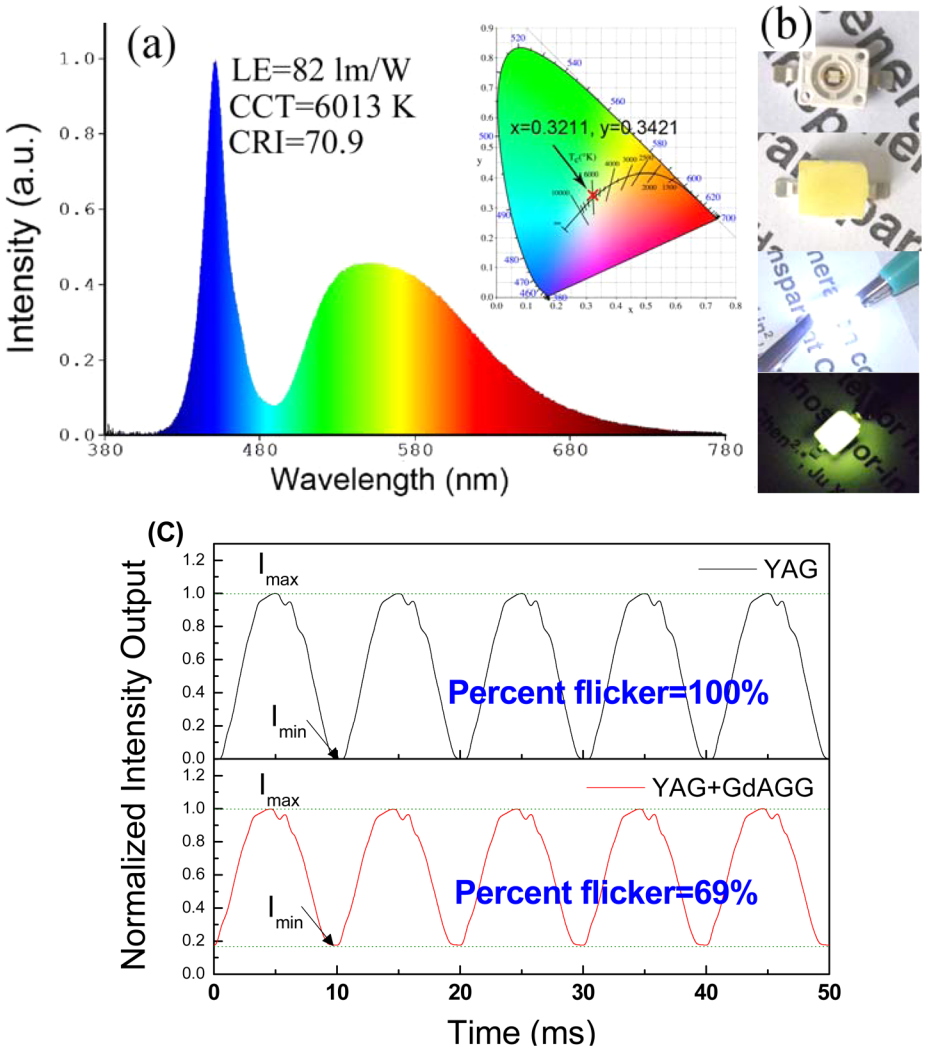

Figure 4. (a) PL spectrum and colorimetry parameters (including LE, CCT, CRI, and chromaticity coordination) of the remote-type AC-LED encapsulated by PiG at an operating current of 350 mA. (b) From top to bottom: photographs of the used blue chip with a groove-shaped sample holder, the assembled LED device covered with PiG on the top, the white luminescence when power is on, the yellowish green afterglow luminescence when power is off. (c) Luminescence intensity variations of the labeled LED devices driven in AC periodic cycles.

Pan.[17] The PPLE spectrum resembles the PLE one, implying the intense afterglow luminescence should be achieved via efficient Ce^{3+} excitation in the blue region. As for the persistent luminescence mechanism (see Figure S4 in the Supporting Information), it is similar to that in Ce^{3+}:$Y_3Al_2Ga_3O_{12}$, which had been fully discussed in Ueda's and our previous paper.[19,20,22] Briefly speaking, blue-light excites the Ce^{3+} 4f electrons to the $5d_1$ level, which can be prompted to the conduction band via photoionization and then captured by the electron traps. These traps should be the Ga-related antisite defects ($Ga_Y^{+\delta}$) or V_{Ga}-Ce^{3+}-V_O defect clusters, and continuously distribute over a wide range of energies.[22,35] The trapped electrons are easily released from the shallower traps, leading to the fast and intense afterglow decay, whereas those escaped from the deeper traps would result in the slow and weak afterglow decay.[36] The persistent behavior of PiG inherits from that of the embedded Ce^{3+}:GdAGG particles.

It is proposed that the intense afterglow luminescence in the microsecond range can be utilized for compensating the AC time gap, whereas the weak one lasting longer can be a good signal indication in emergency when power is shut off without warning. As a proof-of-concept experiment, we fabricated a remote-type AC-LED prototype device based on the PiG (1 mm in thickness) containing 3% commercial Ce^{3+}:YAG and 10% homemade Ce^{3+}:GdAGG, and connected it to an AC bridge circuit (see Figure 4b and Figure S5 in the Supporting Information). As for this "2-phosphor" PiG, one may question the reabsorption of light from one phosphor by the other. We think this effect does exist, but is not very significant because the spectral overlap between excitation and emission in the Ce^{3+}:YAG and Ce^{3+}:GdAGG is small. The QY for this PiG is measured to be 89.4% in Figure S6 in the Supporting Information, only slightly lower than the previously reported 92% in the Ce^{3+}:YAG "1-phosphor" PiG.[9] The thus-fabricated AC-LED device results in a LE of 82 lm/W, a CCT of 6013K, a CRI of 70.9, and a chromaticity coordination of (0.3211, 0.3421), as shown in Figure 4a. It is reasonable that LE decreases from the reported 124 lm/W to the present 82 lm/W, ascribing to the low quantum efficiency of additional Ce^{3+}:GdAGG and the reduced light extraction for semi-transparency of this PiG. However, the value 82 lm/W is still acceptable for general lighting, whereas such PiG yields persistent stimulus intensity favorable for AC-LED application. As shown in Figure 4b, the AC-LED device emits bright white

light when the power is on, and yellowish green afterglow luminescence when the power is off. Although the persistent color is different from the illuminated white color in operation, such color variation in a ~5−20 ms time scale is conceivably not sensitive to human eyes. Thanking to the uniform plane light output, the remote-type AC-LED exhibits lower glare than the conventional LED. To evaluate the ability of the persistent PiG in reducing the flickering effect, the luminescence intensity variation of LED driven in AC periodic cycles is measured, as demonstrated in Figure 4c. As a comparison, the experimental result for an AC-LED based on the PiG containing merely Ce^{3+}:YAG is also presented in Figure 4c. The percent flicker (δ), expressed as $\delta = 100\% \times (I_{max} - I_{min})/(I_{max} + I_{min})$,[37] is adopted to evaluate the flickering effect, where I_{max} and I_{min} represent the maximal and minimal luminescent intensity. As expected, 100% percent flicker is found in the 3% YAG PiG, while only 69% one is found in the 3%YAG+10%GdAGG persistent PiG. It is expected this value could be further reduced by increasing the GdAGG contents (the GdAGG weight ratio dependent percent flicker is shown in Figure S7 in the Supporting Information); however, the glass melt will become too viscous to obtain the PiG. Given there are still 69% difference in intensity from the on state, great efforts should be employed to explore more efficient blue-light-activated persistent phosphors, or possibly some extra circuit design should be performed to modulate the input AC sine wave to square wave.

4. CONCLUSION

In summary, blue-light-activated Ce^{3+}:GdAGG persistent PiGs were successfully developed via a PiG approach for high-powered remote-type white AC-LED application. The XRD and SEM results reveal the glass-melting process has low impact on the microstructure of GdAGG particles, whereas the spectroscopic analysis confirms the spectral features of Ce^{3+} are retained. The persistent luminescent behavior of PiG was carefully examined, showing a fast decay in a microsecond range, which is proposed beneficial to compensating the AC time gap. After coupling the persistent PiG with blue chip and connecting it into bridge AC circuit, the assembled remote-type AC-LED device yields a LE of 82 lm/W, a CCT of 6013K, a CRI of 70.9, and a chromaticity coordination of (0.3211, 0.3421); remarkably, the percent flicker is found to drop from 100 to 69%. Hopefully, the persistent PiG-based AC-LED would be a new-generation lighting source with cheaper price, more robustness, lower flicker, and higher color quality.

■ ASSOCIATED CONTENT

Supporting Information

The transmittance spectrum of glass (1 mm thickness) without introducing Ce^{3+}:GdAGG phosphors (Figure S1). Photoluminescence decay curves and QY measurement of Ce^{3+}:GdAGG powder and GC (Figure S2). The persistent decay curves of xCe^{3+}:GdAGG (x = 0.5, 1.0, 2.0, and 4.0%) PiGs (Figure S3). Schematic illustration of persistent luminescence mechanism in Ce^{3+}:GdAGG GC (Figure S4). Schematic illustration of the used AC bridge circuit (Figure S5). QY measurement for the PiG containing 3% Ce^{3+}:YAG and 10% Ce^{3+}:GdAGG (Figure S6). GdAGG weight ratio (x = 0, 2, 5, and 10%) dependent percent flicker of the fabricated 3%YAG +x%GdAGG PiG based AC-LED devices (Figure S7). This material is available free of charge via the Internet at http://pubs.acs.org.

■ AUTHOR INFORMATION

Corresponding Author

*E-mail: yswang@fjirsm.ac.cn. Tel/Fax: +86-591-83705402.

Notes

The authors declare no competing financial interest.

■ ACKNOWLEDGMENTS

This work was supported by National Natural Science Foundation of China (11204301, 51172231, 21271170, 11304312, 51472242), the Major Sci & Tech Projects of Fujian (2011HZ0001-2), and the key innovation project of Haixi Institute of CAS (SZD13001).

■ REFERENCES

(1) Schubert, E. F.; Kim, J. K. Solid-State Light Sources Getting Smart. *Science* **2005**, *308*, 1274−1278.
(2) Ye, S.; Xiao, F.; Pan, Y. X.; Ma, Y. Y.; Zhang, Q. Y. Phosphors in Phosphor-Converted White Light-Emitting Diodes: Recent Advances in Materials, Techniques and Properties. *Mater. Sci. Eng., R* **2010**, *71*, 1−34.
(3) Smet, P. F.; Parmentier, A. B.; Poelman. Selecting Conversion Phosphors for White Light-Emitting Diodes. D. *J. Electrochem. Soc.* **2011**, *158*, R37−R54.
(4) Žukauskas, A.; Shur, M. S.; Gaska, R. In *Introduction to Solid State Lighting*; John Wiley & Sons: New York, 2002; Chapter 4, pp 37−48.
(5) Höppe, H. A. Recent Developments in The Field of Inorganic Phosphors. *Angew. Chem., Int. Ed.* **2009**, *48*, 3572−3582.
(6) Yeh, C. W.; Li, Y.; Wang, J.; Liu, R. S. Appropriate Green Phosphor of $SrSi_2O_2N_2$: Eu^{2+},Mn^{2+} for AC LEDs. *Opt. Express* **2012**, *20*, 18031−18034.
(7) Chen, L.; Zhang, Y. S.; Xue, C.; Deng, X. R.; Luo, A. Q.; Liu, F. Y.; Jiang, Y. The Green Phosphor $SrAl_2O_4$: Eu^{2+}, R^{3+} (R = Y, Dy) and Its Application in Alternating Current Light-Emitting Diodes. *Funct. Mater. Lett.* **2013**, *6*, 1350047.
(8) Chen, L.; Zhang, Y.; Liu, F. Y.; Luo, A. Q.; Chen, Z. X.; Jiang, Y.; Chen, S. F.; Liu, R. S. A New Green Phosphor of $SrAl_2O_4$: Eu^{2+}, Ce^{3+}, Li^+ for Alternating Current Driven Light-Emitting Diodes. *Mater. Res. Bull.* **2012**, *47*, 4071−4075.
(9) Zhang, R.; Lin, H.; Yu, Y. L.; Chen, D. Q.; Xu, J.; Wang, Y. S. A New-Generation Color Converter for High-Power White LED: Transparent Ce^{3+}:YAG Phosphor-in-Glass. *Laser Photonics Rev.* **2014**, *8*, 158−164.
(10) Lin, H.; Zhang, R.; Chen, D. Q.; Yu, Y. L.; Yang, A. P.; Wang, Y. S. Tuning of Multicolor Emissions in Glass Ceramics Containing γ-Ga_2O_3 and β-YF_3 Nanocrystals. *J. Mater. Chem. C* **2013**, *1*, 1804−1811.
(11) Zhang, X. J.; Huang, L.; Pan, F. J.; Wu, M. M.; Wang, J.; Chen, Y.; Su, Q. Highly Thermally Stable Single-Component White-Emitting Silicate Glass for Organic-Resin-Free White-Light-Emitting Diodes. *ACS Appl. Mater. Interfaces* **2014**, *6*, 2709−2717.
(12) Fulmek, P.; Sommer, C.; Hartmann, P.; Pachler, P.; Hoschopf, H.; Langer, G.; Nicolics, J.; Wenzl, F. P. On The Thermal Load of The Color-Conversion Elements in Phosphor-Based White Light-Emitting Diodes. *Adv. Opt. Mater.* **2013**, *1*, 753−762.
(13) Allen, M. Preferred Embodiment to LED Light String. Patent No. US 20030015968.
(14) Choi, B. H.; Park, I. K.; Kim, D. H. Ac Light Emitting Device, Driving Device Thereof, and Driving Method Thereby. Patent No. WO 2010058923.
(15) van den Eeckhout, K.; Smet, P. F.; Poelman, D. Persistent Luminescence in Eu^{2+}-Doped Compounds: A Review. *Materials* **2010**, *3*, 2536−2566.
(16) Jia, D. D.; Wang, X. J.; Yen, W. M. Delocalization, Thermal Ionization, and Energy Transfer in Singly Doped and Codoped $CaAl_4O_7$ and Y_2O_3. *Phys. Rev. B* **2004**, *69*, 235113.
(17) Pan, Z. W.; Lu, Y. Y.; Liu, F. Sunlight-Activated Long-Persistent Luminescence in The Near-Infrared from Cr^{3+}-Doped Zinc Gallogermanates. *Nat. Mater.* **2012**, *11*, 58−63.

(18) Dorenbos, P. Mechanism of Persistent Luminescence in Eu^{2+} and Dy^{3+} Codoped Aluminate and Silicate Compounds. *J. Electrochem. Soc.* **2005**, *152*, H107−H110.
(19) Ueda, J.; Kuroishi, K.; Tanabe, S. Bright Persistent Ceramic Phosphors of Ce^{3+}-Cr^{3+}-Codoped Garnet Able to Store by Blue Light. *Appl. Phys. Lett.* **2014**, *104*, 101904.
(20) Ueda, J.; Tanabe, S.; Nakanishi, T. Analysis of Ce^{3+} Luminescence Quenching in Solid Solutions between $Y_3Al_5O_{12}$ and $Y_3Ga_5O_{12}$ by Temperature Dependence of Photoconductivity Measurement. *J. Appl. Phys.* **2011**, *110*, 053102.
(21) Ueda, J.; Kuroishi, K.; Tanabe, S. Yellow Persistent Luminescence in Ce^{3+}-Cr^{3+}-Codoped Gadolinium Aluminum Gallium Garnet Transparent Ceramics after Blue-Light Excitation. *Appl. Phys. Express* **2014**, *7*, 062201.
(22) Wang, B.; Lin, H.; Yu, Y. L.; Chen, D. Q.; Zhang, R.; Xu, J.; Wang, Y. S. Ce^{3+}/Pr^{3+}:YAGG: A Long Persistent Phosphor Activated by Blue-Light. *J. Am. Ceram. Soc.* **2014**, *97*, 2539−2545.
(23) Fujita, S.; Sakamoto, A.; Tanabe, S. Luminescence Characteristics of YAG Glass-Ceramic Phosphor for White LED. *IEEE J. Sel. Top. Quantum Electron.* **2008**, *14*, 1387−1391.
(24) Nakanishi, T.; Tanabe, S. Novel Eu^{2+}-Activated Glass Ceramics Precipitated With Green and Red Phosphors for High-Power White LED. *IEEE J. Sel. Top. Quantum Electron.* **2009**, *15*, 1171−1176.
(25) Lee, J. S.; Arunkumar, P.; Kim, S.; Lee, I. J.; Lee, H.; Im, W. B. Smart Design to Resolve Spectral Overlapping of Phosphor-in-Glass for High-Powered Remote-Type White Light-Emitting Devices. *Opt. Lett.* **2014**, *39*, 762−765.
(26) Lee, Y. K.; Lee, J. S.; Heo, J.; Im, W. B.; Chung, W. J. Phosphor in Glasses with Pb-Free Silicate Glass Powders as Robust Color-Converting Materials for White LED Applications. *Opt. Lett.* **2012**, *37*, 3276−3278.
(27) Chen, L. Y.; Cheng, W. C.; Tsai, C. C.; Huang, Y. C.; Lin, Y. S.; Cheng, W. H. High-Performance Glass Phosphor for White-Light-Emitting Diodes via Reduction of Si-Ce^{3+}:YAG Inter-Diffusion. *Opt. Mater. Express* **2014**, *4*, 121−128.
(28) Segawa, H.; Ogata, S.; Hirosaki, N.; Inoue, S.; Shimizu, T.; Tansho, M.; Ohki, S.; Deguchi, K. Fabrication of Glasses of Dispersed Yellow Oxynitride Phosphor for White Light-Emitting Diodes. *Opt. Mater.* **2010**, *33*, 170−175.
(29) Zhu, Y. T.; Nadarajah, N. Investigation of Remote-Phosphor White Light-Emitting Diodes with Multi-Phosphor Layers. *Jpn. J. Appl. Phys.* **2010**, *49*, 100203.
(30) Luo, H.; Kim, J. K.; Schubert, E. F.; Cho, J.; Sone, C.; Park, Y. Analysis of High-Power Packages for Phosphor-Based White-Light-Emitting Diodes. *Appl. Phys. Lett.* **2005**, *86*, 243505.
(31) Won, Y. H.; Jang, H. S.; Cho, K. W.; Song, Y. S.; Jeon, D. Y.; Kwon, H. K. Effect of Phosphor Geometry on The Luminous Efficiency of High-Power White Light-emitting Diodes with Excellent Color Rendering Property. *Opt. Lett.* **2009**, *34*, 1−3.
(32) Xu, Y. S.; Zhang, X. H.; Dai, S. X.; Fan, B.; Ma, H. L.; Adam, J. L.; Ren, J.; Chen, G. R. Efficient Near-Infrared Down-Conversion in Pr^{3+}−Yb^{3+} Codoped Glasses and Glass Ceramics Containing LaF_3 Nanocrystals. *J. Phys. Chem. C* **2011**, *115*, 13056.
(33) Blasse, G.; Bril, A. A New Phosphor for Flying-Spot Cathode-Ray Tubes for Color Television: Yellow-Emitting $Y_3Al_5O_{12}$-Ce^{3+}. *Appl. Phys. Lett.* **1967**, *11*, 53−55.
(34) Fang, Z. J.; Cao, R. P.; Zhang, F. T.; Ma, Z. J.; Dong, G. P.; Qiu, J. R. Efficient Spectral Conversion from Visible to Near-Infrared in Transparent Glass Ceramics Containing Ce^{3+}−Yb^{3+} Codoped $Y_3Al_5O_{12}$ Nanocrystals. *J. Mater. Chem. C* **2014**, *2*, 2204−2211.
(35) Piegza, J. T.; Niittykoski, J.; Hölsä, J.; Zych, E. Thermoluminescence and Kinetics of Persistent Luminescence of Vacuum-Sintered Tb^{3+}-doped and Tb^{3+},Ca^{2+}-Codoped Lu_2O_3 Materials. *Chem. Mater.* **2008**, *20*, 2252−2261.
(36) Li, Y.; Zhou, S. F.; Dong, G. P.; Peng, M. Y.; Wondraczek, L.; Qiu, J. R. Anti-Stokes Fluorescent Probe with Incoherent Excitation. *Sci. Rep.* **2014**, *4*, 4059.
(37) *The IESNA Lighting Handbook*, 9 th ed.; Rea, M. S., Ed.; Illuminating Engineering Society: New York, 2000; Chapter 2, pp 44−87.